American Journal of Analytical Chemistry, 2014, 5, 695-700
Published Online August 2014 in SciRes. http://www.scirp.org/journal/ajac
http://dx.doi.org/10.4236/ajac.2014.511078

Structural and Thermal Properties of Tb, Ce Doped $Y_{2.97}Gd_{0.03}Al_2Ga_3O_{12}$ Single Crystals

Mohammad Faheem*, Kelvin Lynn

Center for Materials Research, Washington State University, Pullman, WA, USA
Email: *faheem2001@gmail.com

Received 23 May 2014; revised 9 July 2014; accepted 25 July 2014

Abstract

The structural and thermal properties of yttrium-aluminum-gadolinium-gallium ($Y_{2.97}Gd_{0.03}Al_2Ga_3O_{12}$) single crystals doped with terbium (0.1%), cerium (0.01%) and co-doped with both terbium and cerium ((0.1, 0.01)%) were investigated. All samples were heated (calcined) at 1400˚C for 15 hours before crystallization. X-ray powder diffraction (XRD) patterns of all calcined samples showed the presence of yttrium gallium aluminate ($Y_3Al_2Ga_3O_{12}$) and gadolinium gallium oxide (Gd_3GaO_6) while the grown crystals were single phase of $Y_3Al_2Ga_3O_{12}$. The lattice parameter of the crystals decreased with Ce doping. The thermal conductivity of each sample was determined from 25˚C to 300˚C and found to decrease exponentially with increasing temperature. All doped crystals have different thermal conductivity, which is attributed to the crucial influence of crystals structures. 0.01% Ce:YAGG was found to be a strong candidate for scintillators and other lasing materials because of its good thermal behavior (10.71 W/m·K).

Keywords

YAGG Single Crystals, Lattice Parameters, Thermal Conductivity

1. Introduction

Garnet-based single crystals are widely used in several applications such as solid state lighting, scintillators and fluorescent displays because of their high thermal conductivity and excellent physical and chemical properties [1]-[3]. The stoichiometric formula for garnet structures is $\{A_3\}$ $[B_2]$ (C_3) O_{12}, where { }, [ ] and ( ) represent the dodecahedral, octahedral and tetrahedral sites in the lattice. All of these atomic positions are fixed by symmetry. Garnets possess cubic structures but there are some experimental results suggesting that garnet structures deviate from cubic symmetry [4]. Some important properties of garnets include hardness, lasing, magnetic magne-

*Corresponding author.

to-optical behavior, radiation detection and thermal conductivity [5]-[7]. Among these, thermal properties are one of most important concerns when designing a crystal. Up to now YAG and GGG series of crystals have received great attention due to their large size and reasonable thermal behavior. For example, Nd:YAG, Yb:YAG, Nd:GGG, and Yb:GGG crystals have been obtained by the Czochralski method [8] [9]. It has been previously reported that thermal conductivity (κ) observed for undoped YAG is 10.3 and for undoped GGG it is 8 W/m·K at 300 K [10] and the value of κ decreases depending upon the nature and quantity of dopants [9] [11]. Finally, owing to such wide and diverse application of garnet-based structures, the demand for new garnet crystals will continue to exist.

Rare earth materials have been widely used due to their unique characteristics such as high refractive index, thermal stability, fluorescence, catalytic etc. Cerium is one of the most significant rare-earth materials which exhibits high catalytic behavior and is used in several applications such as light emission treatment where it has shown great potential [1] [12]. Cerium oxide is known to form stable solid solution with other rare-earth oxides [13]. On the other hand, terbium has high density (8.26 g/cm^3) compared to cerium (6.77 g/cm^3), exhibits good luminescence property and can form fluorescent complexes with a wider variety of materials [14]. Such properties make the cerium and terbium highly demanded for future materials.

In this work, we have synthesized single crystals of YAGG doped with Ce and Tb to determine how doping affects the lattice parameters and thermal properties in the range of 25˚C to 300˚C. We have determined the lattice parameters, thermal diffusivity and specific heat; and thermal conductivity is a function of different temperatures and doping.

2. Experimental Details

Ceramic powders Y_2O_3, Al_2O_3, Ga_2O_3, and Gd_2O_3 possessed 4N-5N purity were purchased from commercial vendors. Cerium Carbonate Hydrate ($Ce_2(CO_3)_3{\cdot}XH_2O$) and Terbium Carbonate Hydrate ($Tb_2(CO_3)_3{\cdot}XH_2O$) were chosen as dopants.

Doped $Y_{2.97}Gd_{0.03}Al_2Ga_3O_{12}$ charges were prepared with the stoichiometry of pure garnet phase.

The cerium and terbium concentrations were kept at 0.01 and 0.1 atomic percentage, respectively, while preparing the charges. Three samples were prepared: 0.01% Ce doped YAGG; 0.1% Tb doped YAGG; and co-doped (0.01, 0.1)% Ce, Tb:YAGG. All materials were individually weighed and mixed in a Glass-Col® mixer for 2 hours. The mixture was then isostatically pressed to ~20 kpsi to form a pellet of ~86 mm in diameter and 56 mm in length. The resulting pellet was sintered (calcined) in an alumina crucible at 1400˚C for 15 hours in air.

The calcined charge was then loaded into a cylindrical iridium crucible for crystal growth. The height of crucible was adjusted with respect to the RF coil in order to obtain maximum temperatures. Vertical gradient freeze (VGF) technique in a RF Induction furnace was used for crystal growth. Zirconia insulation was placed between the RF coil and iridium crucible to create a suitable thermal gradient. The power of the furnace was controlled by Eurotherm® controller with a feedback control. All temperatures and furnace power were controlled and measured using fieldpoint modules though the Labview® program. The chamber was evacuated up to 10^{-3} Torr using a conventional mechanical pump and flushed several times with argon. During crystal growth, argon pressure of 2 - 3 psi was maintained to reduce contamination. After the charge melted at 1900˚C, it was cooled to room temperature. The cooling rates varied from 3 - 10˚C/hour from the start of the crystallization until the temperature reached around 1550˚C when the melt become solid. Then ingot was cooled to room temperature at 100 - 120˚C/hour.

X-ray diffraction was employed to identify the phases of calcined charge and crystal parameters. The doped YAGG crystals were characterized by X-ray powder analysis with a Siemens D-500® powder diffractometer equipped a conventional X-ray tube using CuKα radiations with a power condition of 36 kV, 30 mA and step of 0.02˚. The samples for thermal diffusivity measurements were cut from the doped YAGG crystals with the dimensions of 10 mm × 10 mm × 2 mm. The thermal diffusivity and specific heat capacity (C_p) measurements were carried out by the flash method (LFA 447 nanoflash, NETZSCH®) and differential scanning calorimetry (PC 409, STA NETZSCH®). The densities of the crystals were measured using the Archimedes method.

3. Results and Discussion

X-ray diffraction patterns of 0.01% Ce:YAGG calcined and crystal are shown in **Figure 1**. The calcined 0.01%

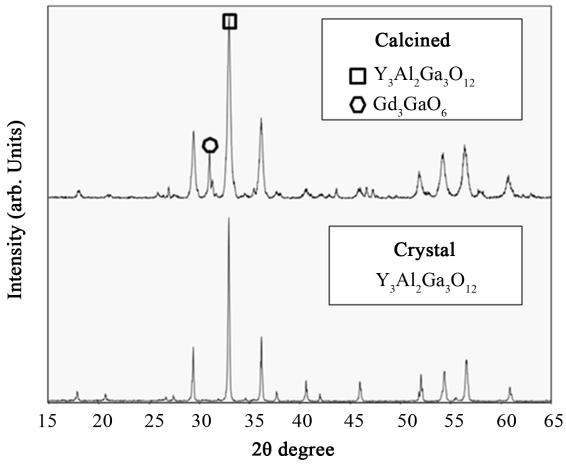

Figure 1. XRD pattern of 0.01% Ce doped YAGG, calcined at 1400˚C and crystal.

Ce:YAGG showed the presence of Gd_3GaO_6 and $Y_3Al_3Ga_3O_{12}$. The presence of Gd_3GaO_6 was 3.5 by volume phase percentage as compared to $Y_3Al_3Ga_3O_{12}$. However, crystal diffraction pattern showed the single phase of cubic garnet $Y_3Al_2Ga_3O_{12}$. This indicates either Gd_3GaO_6 evaporated and was present in less quantity or formed solid solution during crystallization process. All samples showed the same behavior except a shift on the 2θ scale which indicated a change in lattice parameters. This shift in 2θ was measured by the Si Standard Reference Material 640b provided by National Institute of Standards and Technology. The diffraction patterns were easily indentified and corresponded to the standard PDF's [15] [16] using CrystalMaker$^{TM®}$ software. The lattice parameters of the PDF's were decreased by 0.1% for the comparison in **Figure 1** so that full width at half maximum intensity of major peaks matched well corresponding to the experimental values.

The lattice parameters of YAGG crystals as a function of cerium and terbium doping concentrations are shown in **Figure 2**. The lattice parameter increases with Tb doping. We suggest the presence of dopants form homogenous disorders due to defect, vacancies and/or stacking faults in the garnet structure which can cause the change in lattice parameters.

The variations in thermal diffusivity with the temperature of doped YAGG single crystals are shown in **Figure 3**. The thermal diffusivity decreases as temperature increases and its reduction is slower at higher temperatures. The thermal diffusivity of 0.1% Tb doped YAGG crystal at 25˚C was 2.696×10^{-6} m^2/s and it reduced to as much as 51% to 1.36×10^{-6} m^2/s at 300˚C. **Figure 3** also demonstrates the small effect of cerium and terbium doping on thermal diffusivity. The values of thermal diffusivity at 25˚C for co-doped (0.01, 0.1)% Ce, Tb:YAGG and 0.01% Ce:YAGG single crystals were 2.714×10^{-6} and $2.77 \times 10^{-6} \pm 0.005 \times 10^{-6}$ m^2/s, respectively. The thermal diffusivity increases by increasing cerium concentration and there is slight change of thermal diffusivity between Tb:YAGG and Ce, Tb:YAGG single crystals but a prominent change is observed in Ce:YAGG single crystals.

Figure 4 demonstrates the dependence of specific heat of doped YAGG crystals on the temperature. From the figure, it is clear that specific heat increases with temperature for all doped samples. Cerium and terbium doping concentration lead to the change in specific heat within the experiment temperature. The specific heat of 0.1% Tb:YAGG crystal shows lowest specific heat and approximately 76% change in specific heat is observed in the temperature range of 25˚C to 300˚C. The results show the cerium doping concentration has significant influence on the specific heat of YAGG single crystal.

The thermal conductivity (K) was calculated as:

$$K = \rho\alpha C_p$$

where is the density ρ, α is the thermal diffusivity and C_p is the specific capacity.

The densities of 0.1% Tb:YAGG, 0.01% Ce:YAGG and (0.1, 0.01)% Tb, Ce:YAGG were 5.25, 5.24 and 5.25 ± 0.01 gm/cm^3, respectively. The thermal conductivity of doped YAGG single crystals at different temperatures calculated using Equation (1) is shown in **Figure 5**. We can see the affect of doping concentration of cerium and

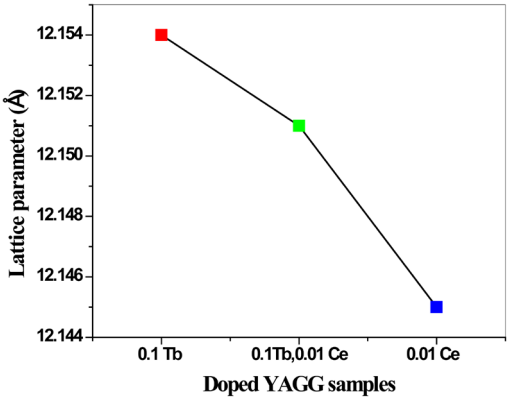

Figure 2. Lattice parameters (Å) of YAGG crystals as function of Tb and Ce doping.

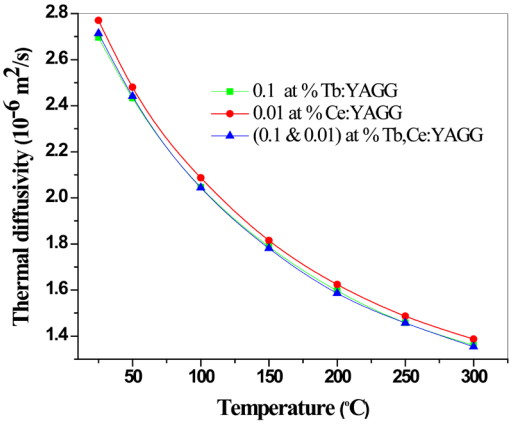

Figure 3. Thermal diffusivity of YAGG single crystal as a function of temperature for doping concentrations.

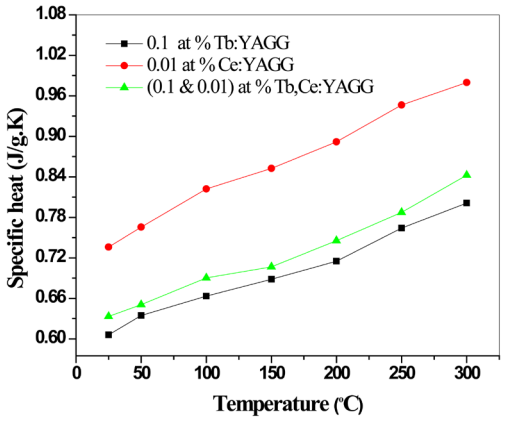

Figure 4. Specific heat of YAGG single crystals as function of temperatures for doping concentrations.

terbium on thermal conductivity. The thermal conductivity of the YAGG single crystal decreases with the increase of temperature. The thermal conductivity of 0.01% Ce:YAGG crystal observed is 10.71 W/m·K which is higher than YAG (10.3 W/m·K) and GGG (8 W/m·K). The value of thermal conductivity decreases as much 16% when 0.1% Tb is added. The thermal conductivity of 0.1% Tb:YAGG crystal is 20% lower than 0.01% Ce:YAGG

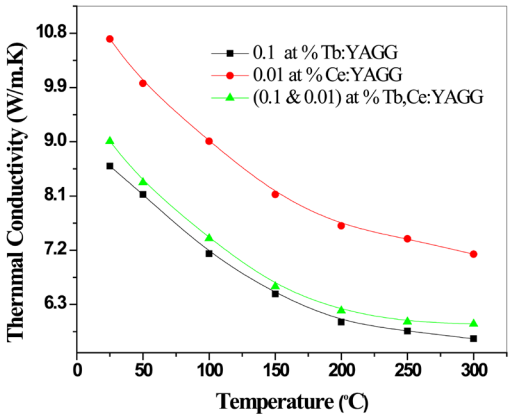

Figure 5. Thermal conductivity of YAGG single crystal results. Tb:YAGG, Ce:YAGG, Tb, Ce:YAGG.

crystal. Hence, thermal conductivity of YAGG single crystals depends upon cerium and terbium doping concentrations and increase in temperature.

Since the crystals studied are nonmetallic and carry no free electrons, the heat is transported predominantly by phonons and photons. The theoretical expression for thermal conductivity is

$$k = \frac{1}{3} c_v \lambda \bar{v} \tag{2}$$

where c_v is the constant volume specific heat, λ is the phonon mean free path, and $\bar{v}$ is the average sound velocity. The c_v of material remains constant until Debye temperature but phonon mean free path and sound velocity are temperature dependent. Phonon mean free path dependence on temperature is approximately

$$\lambda \propto e^{\Theta D/bT} \left(T \ll \Theta_D\right) \tag{3}$$

$$\lambda \propto \frac{1}{T} \left(T \gg \Theta_D\right) \tag{4}$$

where Θ_D is Debye temperature, "*b*" is constant between 2 and 3, and *T* is absolute temperature. The Debye temperatures of the crystals studied are unknown. Our experimental results satisfy the exponential form of Equation (3); hence, heat transportation in our case is predominately due to phonons mean free path below Debye temperature. When temperature increases phonon mean free path decreases which reduces the thermal conductivity as shown in **Figure 5**.

As previously mentioned, the thermal conductivity of YAGG single crystals reduced after doping with Tb^{3+} and increased with Ce^{3+} doping. In garnet structure, a larger ion located at dodecahedral sites such as yttrium in $Y_3Al_3Ga_3O_{12}$ is a medium size ion at octahedral sites and a relatively small ion at tetrahedral sites. The atomic weight of Tb^{3+}, Ce^{3+}, and Y^{3+} are 158.925, 140.25, and 88.905, respectively, and the ionic radius of Tb^{3+}, Ce^{3+}, and Y^{3+} are 0.0923, 0.1034, and 0.0900 nm, respectively. The atomic weight and ionic radius of Tb and Ce are larger than Y. Thus, Tb and Ce are expected to contribute with Y on dodecahedral sites. As can be expected, the much heavier ions are less mobile since Cerium has a larger ionic radius and a less soluble in garnet structure [17]. Hence, the dopants introduce defects and/or oxide stoichiometry in the structure of YAGG single crystals strain which cause a change in lattice parameter as reported in **Figure 2** and ultimately affect the other parameters such as thermal conductivity as observed in **Figure 5**.

4. Conclusion

The lattice parameters and thermal conductivity YAGG single crystals with cerium and terbium concentration were studied. All samples possessed single phase of $Y_3Al_2Ga_3O_{12}$. Thermal diffusivity, specific heat and conductivity were measured from 25˚C to 300˚C. The experimental results indicated that thermal conductivity follows an exponential change. The curve of conductivity declined when adding terbium concentration resulted in a lat-

tice strained. A small change in lattice parameters and thermal conductivity was observed when Ce and Tb were added to YAGG but large change was noticed when only Ce was added to YAGG single crystal. The thermal conductivity curves based on temperatures are mainly due to phonons mean free path and lattice distortion.

Acknowledgements

The authors would like to thank Dr. Marc Weber and Denys Solodovnikov for crystal growth. This work is supported by the National Science Foundation/Department of Homeland Security Domestic Nuclear Detection Office, Academic Research Initiative, under grant number NSF initial grant ECCS-0833275/DHS continuation grants 2009-DN-077-ARI029-02 and 2009-DN-077-ARI029-03 and is highly appreciated.

References

[1] Wu, J.L., Gundiah, G. and Cheetham, A.K. (2007) Structure-Property Correlations in Ce Doped Garnet Phosphors for Use in Solid State Lighting. *Chemical Physics Letters*, **441**, 250-254. http://dx.doi.org/10.1016/j.cplett.2007.05.023

[2] Solodovnikov, D., Weber, M.H. and Lynn, K.G. (2008) Improvement of Scintillation Performance of Ce, Er Codoped Yttrium Aluminum Crystal by Means of Post Growth Treatment. *Applied Physics Letters*, **93**, Article ID: 104102. http://dx.doi.org/10.1063/1.2981086

[3] Xia, G., Zhou, S., Zhang, J. and Xu, J. (2005) Structural and Optical Properties of YAG:Ce^{3+} Phosphors by Sol-Gel Combustion Method. *Journal of Crystal Growth*, **279**, 357-362. http://dx.doi.org/10.1016/j.jcrysgro.2005.01.072

[4] Dillon Jr., J.F. (1958) Optical Properties of Several Ferrimagnetic Garnets. *Journal of Applied Physics*, **29**, 539-541. http://dx.doi.org/10.1063/1.1723215

[5] Hansen, P. and Krumme, J.-P. (1984) Magnetic and Magneto-Optical Properties of Garnet Films. *Thin Solid Films*, **114**, 69-107. http://dx.doi.org/10.1016/0040-6090(84)90337-7

[6] Hansen, P., Witter, K. and Tolksdorf, W. (1983) Magnetic and Magneto-Optic Properties of Lead- and Bismuth-Substituted Yttrium Iron Garnet Films. *Physical Review B*, **27**, 6608-6625. http://dx.doi.org/10.1103/PhysRevB.27.6608

[7] Zorenko, Yu., Gorbenkoa, V., Konstankevych, I., Grinev, B. and Globus, M. (2002) Scintillation Properties of $Lu_3Al_5O_{12}$:Ce Single-Crystalline Films. *Nuclear Instruments and Methods in Physics Research*, **486**, 309-314. http://dx.doi.org/10.1016/S0168-9002(02)00725-8

[8] Chénais, S., Druon, F., Balembois, F., Georges, P., Brenier, A. and Boulon, G. (2003) Diode-Pumped Yb:GGG Laser: Comparison with Yb:YAG. *Optical Materials*, **22**, 99-106. http://dx.doi.org/10.1016/S0925-3467(02)00353-1

[9] Wang, B.S., Jiang, H.H., Zhang, Q.L. and Yin, S. (2007) Thermal Conductivity of Synthetic Garnet Laser Crystals. *The European Physical Journal—Applied Physics*, **39**, 23-26. http://dx.doi.org/10.1051/epjap:2007091

[10] Slack, G.A. and Oliver, D.W. (1971) Thermal Conductivity of Garnets and Phonon Scattering by Rare-Earth Ions. *Physical Review B*, **4**, 592-609. http://dx.doi.org/10.1103/PhysRevB.4.592

[11] Wang, B., Jiang, H., Jia, X., Zhang, Q., Sun, D. and Yin, S. (2008) Thermal Conductivity of Doped YAG and GGG Laser Crystal. *Frontiers of Optoelectronics in China*, **1**, 138-141. http://dx.doi.org/10.1007/s12200-008-0049-6

[12] Blasse, G. and Bril, A. (1967) Investigation of Ce^{+3}-Activated Phosphors. *The Journal of Chemical Physics*, **47**, 5139-5145. http://dx.doi.org/10.1063/1.1701771

[13] Etsell, T.H. and Flengas, S.N. (1970) Electrical Properties of Solid Oxide Electrolytes. *Chemical Review*, **70**, 339-376. http://dx.doi.org/10.1021/cr60265a003

[14] Gao, X.C., Cao, H., Haung, C. and Li, B. (1998) Electroluminescence of a Novel Terbium Complex. *Applied Physics Letters*, **72**, 2217-2219. http://dx.doi.org/10.1063/1.121327

[15] Yamane, H., Sakamoto, T., Kubota, S. and Shimada, M. (1999) X-Ray Powder Diffraction. *Acta Crystallographica Section C*, **55**, 479-481.

[16] Nakatsuka, A., Yoshiasa, A. and Yamanaka, T. (1999) Cation Distribution and Crystal Chemistry of $Y_3Al_{5-x}Ga_xO_{12}$ ($0 \le x \le 5$) Garnet Solid Solutions. *Acta Crystallographica Section B*, **55**, 266-272. http://dx.doi.org/10.1107/S0108768198012567

[17] Saladino, M.L., Caponetti, E., Chillura, D., Enzo, S. and Ibba, G. (2008) Effect of the Dopant Selection (Er, Eu, Nd or Ce) and Its Quantity on the Formation of Yttrium Aluminum Garnet Nanopowders. *Optics Materials*, **31**, 261-267. http://dx.doi.org/10.1016/j.optmat.2008.04.008

Scientific Research Publishing (SCIRP) is one of the largest Open Access journal publishers. It is currently publishing more than 200 open access, online, peer-reviewed journals covering a wide range of academic disciplines. SCIRP serves the worldwide academic communities and contributes to the progress and application of science with its publication.

Other selected journals from SCIRP are listed as below. Submit your manuscript to us via either submit@scirp.org or Online Submission Portal.